Molecular Biology of the Cell
Vol. 19, 5593–5603, December 2008

Ca^{2+}-regulated Pool of Phosphatidylinositol-3-phosphate Produced by Phosphatidylinositol 3-Kinase C2α on Neurosecretory Vesicles

Peter J. Wen,* Shona L. Osborne,* Isabel C. Morrow,† Robert G. Parton,† Jan Domin,‡ and Frederic A. Meunier*

*Molecular Dynamics of Synaptic Function Laboratory, Queensland Brain Institute and School of Biomedical Sciences, The University of Queensland, St. Lucia, 4072 Queensland, Australia; † Centre for Microscopy and Microanalysis and Institute for Molecular Bioscience, University of Queensland, Brisbane, Queensland 4072, Australia; and ‡Renal Section, Faculty of Medicine, Imperial College, London W12 0NN, United Kingdom

Submitted June 12, 2008; Revised September 15, 2008; Accepted September 30, 2008
Monitoring Editor: Sean Munro

Phosphatidylinositol-3-phosphate [PtdIns(3)P] is a key player in early endosomal trafficking and is mainly produced by class III phosphatidylinositol 3-kinase (PI3K). In neurosecretory cells, class II PI3K-C2α and its lipid product PtdIns(3)P have recently been shown to play a critical role during neuroexocytosis, suggesting that two distinct pools of PtdIns(3)P might coexist in these cells. However, the precise characterization of this additional pool of PtdIns(3)P remains to be established. Using a selective PtdIns(3)P probe, we have identified a novel PtdIns(3)P-positive pool localized on secretory vesicles, sensitive to PI3K-C2α knockdown and relatively resistant to wortmannin treatment. In neurosecretory cells, stimulation of exocytosis promoted a transient albeit large increase in PtdIns(3)P production localized on secretory vesicles sensitive to PI3K-C2α knockdown and expression of PI3K-C2α catalytically inactive mutant. Using purified chromaffin granules, we found that PtdIns(3)P production is controlled by Ca^{2+}. We confirmed that PtdIns(3)P production from recombinantly expressed PI3K-C2α is indeed regulated by Ca^{2+}. We provide evidence that a dynamic pool of PtdIns(3)P synthesized by PI3K-C2α occurs on secretory vesicles in neurosecretory cells, demonstrating that the activity of a member of the PI3K family is regulated by Ca^{2+} in vitro and in living neurosecretory cells.

INTRODUCTION

Phosphatidylinositol-3-phosphate [PtdIns(3)P] can be produced by the activity of a variety of phosphatidylinositol 3-kinases (PI3Ks) (Gillooly *et al*., 2000) and phosphatidylinositol phosphatases (Kong *et al*., 2006). In mammalian cells, one of the major pools of PtdIns(3)P is mainly produced by class III PI3-kinase (hvps34p) on early endosomes and multivesicular bodies (Gillooly *et al*., 2000). In yeast, PtdIns(3)P has been implicated in traffic from the *trans*-Golgi network to vacuoles via endosomes and multivesicular bodies (Corvera and Czech, 1998; Corvera *et al*., 1999). In mammalian cells, most PtdIns(3)P production occurs on early endosomes and is critical for endosomal fusion—a process tightly regulated by Rab5 activity (Christoforidis *et al*., 1999).

Emerging evidence has suggested that 3-phosphorylated phosphoinositides could play a critical role in the early steps of exocytosis (Osborne *et al*., 2001, 2006; Cousin *et al*., 2003; Meunier *et al*., 2005; Lindmo and Stenmark, 2006). However, the potential role of PI3Ks in exocytosis has been controversial (Milosevic *et al*., 2005), in part due to the relative insensitivity of the exocytic process to the classical PI3K inhibitors wortmannin and LY294002 (Chasserot-Golaz *et al*., 1998). Class II PI3K-C2α (PI3K-C2α) is relatively insensitive to PI3K inhibitors compared with all other PI3K enzymes (Domin *et al*., 1997). Recent evidence suggested that PI3K-C2α is localized on secretory vesicles and able to modulate ATP-dependent priming of large dense core vesicles (LDCVs) through its kinase activity, suggesting a potential role for PtdIns(3)P in exocytosis (Meunier *et al*., 2005). More insight into PtdIns(3)P function in neurosecretory cells came with the demonstration that PtdIns(3)P sequestration via the selective binding of the tandem FYVE domain, $2xFYVE^{Hrs}$ domain, blocked neurosecretion in chromaffin and pheochromocytoma (PC12) cells (Meunier *et al*., 2005). This raised a number of questions regarding the localization of PtdIns(3)P production and the specific pathways involved in PtdIns(3)P synthesis in neurosecretory cells.

Because PI3K-C2α is located on neurosecretory granules (Meunier *et al*., 2005), it is likely that neurosecretory cells might have several ways of synthesizing PtdIns(3)P in distinct subcellular compartments. This point is supported by recent work implicating PIKfyve in negatively regulating neuroexocytosis through the phosphorylation of PtdIns(3)P to produce phosphatidylinositol 3,5-bisphosphate [$PtdIns(3,5)P_2$] (Osborne *et al*., 2008).

In the current study, we found that neurosecretory cells contain two major pools of PtdIns(3)P, one located on early endosomes, sensitive to wortmannin inhibition, and the other located on a subpopulation of LDCVs and relatively insensitive to wortmannin. We found that PI3K-C2α activity was greatly enhanced by Ca^{2+} and revealed that PtdIns(3)P production on

This article was published online ahead of print in *MBC in Press* (http://www.molbiolcell.org/cgi/doi/10.1091/mbc.E08–06–0595) on October 8, 2008.

Address correspondence to: Frederic A. Meunier (f.meunier@uq.edu.au).

LDCVs was significantly and transiently increased during stimulation of exocytosis in neurosecretory cells.

MATERIALS AND METHODS

Chromaffin Cell Preparation

Bovine adrenal chromaffin cells were isolated as described previously (Meunier *et al*., 2005) and cultured in DMEM supplemented with 10% fetal bovine serum. The cells were maintained at 37°C in 5% CO_2 incubator for at least 24 h before use in experiments.

Transfection

PC12 cells and human embryonic kidney (HEK) cells growing on (poly-lysine–treated coverslips were transfected using Lipofectamine LTX (Invitrogen, Carlsbad, CA) according to manufacturer's instructions. Cells were processed for immunocytochemistry or time-lapse confocal microscopy imaging 15–24 h after transfection.

Immunocytochemistry

Cells plated on poly-D-lysine–coated coverslips for 15–24 h, were briefly washed with buffer A: 145 mM NaCl, 5 mM KCl, 1.2 mM Na_2HPO_4, 10 mM glucose, and 20 mM HEPES-NaOH, pH 7.4, and fixed with 4% paraformaldehyde (PFA) for 30 min. In some experiments, transfected cells were pretreated with stated concentrations of wortmannin (Sigma-Aldrich, New Castle, NSW, Australia) for 25–30 min before fixation. For digitonin permeabilization, cells were incubated with 20 μM digitonin in KGEP buffer: 139 mM K-glutamate, 5 mM glucose, 5 mM EGTA, and 20 mM piperazine-*N*,*N*′-bis(2-ethanesulfonic acid) (PIPES)-NaOH, pH 6.7, containing 2 mM free Mg^{2+} and 2 mM ATP in the continuing presence of 2xFYVE-glutathione transferase (GST) (17 μM; a kind gift from G. Schiavo, Cancer Research UK) for 10 min. The cells were briefly washed in KGEP buffer, fixed with 4% PFA, and processed for immunocytochemistry. Coverslips were blocked using blocking buffer (3% normal horse serum, 0.5% bovine serum albumin (BSA), and 0.05% Triton X-100) before incubation with the primary antibodies (anti-GST polyclonal antibody; Sigma-Aldrich), anti-synaptotagmin 1 (M48; a kind gift from G. Schiavo; Matthew *et al*., 1981), anti-early endosomal antigen 1 (BD Biosciences, San Jose, CA) and anti-P18 (a kind gift from S. Tooze, Cancer Research UK, London, United Kingdom). After washing with phosphate-buffered saline (PBS), coverslips were incubated with Alexa 488- and Alexa 546-conjugated secondary antibodies (Invitrogen), washed with PBS, and mounted (Prolong Gold; Invitrogen). Images were examined by confocal microscopy (LSM 510 Meta; Carl Zeiss, Jena, Germany). Quantification of the degree of colocalization was carried out using the color range tool in the LSM510 software. Briefly, immunopositive puncta were selected (pixel intensity >100 arbitrary units) solely in the green channel as regions of interests (by switching off the red channel). Twelve to 132 regions of interests were selected per cell for at least nine cells. By adjusting the red channel (pixel intensity >100 arbitrary units), the organelles showing a high degree of colocalization in the merged image were scored over those that did not colocalize and are expressed as a percentage.

Subcellular Fractionation of Chromaffin Cells

Chromaffin granules were prepared as described previously (Bon *et al*., 1990; Vitale *et al*., 1996; Meunier *et al*., 2005; Osborne *et al*., 2007). Briefly, bovine adrenal medulla were taken and finely chopped in 0.32 M sucrose (10 mM Tris, 1 mM EGTA, pH 7.4, and protease inhibitor [Roche Products, Dee Why, NSW, Australia]). Medullas were homogenized and centrifuged at 800 × *g* for 15 min. After filtering of the supernatant, filtrates were centrifuged at 12,000 × *g* for 20 min. Pellets were resuspended in 0.32 M sucrose, layered on a 1.6 M sucrose gradient, and centrifuged 1 h at 127,000 × *g*. Pink chromaffin granules pellet fraction collected and analyzed for its concentration by Bradford assay.

Chromaffin Granules Kinase Assay and Lipid Analysis

Frozen purified chromaffin granules were slowly thawed on ice. In each assay, 300 μg of chromaffin granules were used. Chromaffin granules were diluted in KGEP buffer containing 2 mM $MgCl_2$, protease inhibitor with or without bovine adrenal medulla cytosol (500 μg) (Panaretou and Tooze, 2002), 2 mM ATP, and indicated concentrations of $CaCl_2$, pH 6.8. After 30 min at 37°C, the reactions were stopped by mixing with 1 M HCl. Lipids were extracted by addition of chloroform ($CHCl_3$):methanol (MeOH) (1:1, vol/vol) and 2 M KCl to the acidified samples. The lower organic phase was collected and dried under a low stream of N_2. Dried lipids were resuspended in chloroform and spotted on oxalate-treated thin layer chromatography (TLC) plates. For control experiment, synthetic phosphoinositides PtdIns(3)P, phosphatidylinositol-4-phosphate [PtdIns(4)P], phosphatidylinositol-5-phosphate [PtdIns(5)P], PtdIns(3,5)P_2, phosphatidylinositol 3,4-bisphosphate [PtdIns(3,4)P_2], and phosphatidylinositol 3,4,5-triphosphate [PtdIns(3,4,5)P_3] (diC16, acid form) (Cell Signals, Columbus, OH) were dried and resuspended in chloroform and spotted on oxalate-treated TLC plates. Lipids were separated on TLC plates in a pre-equilibrated tank containing $CHCl_3$:MeOH: distilled H_2O:NH_4OH (30%) (9:7:1:1, vol/vol). TLC plates were dried overnight before processing for overlay assay.

For overlay assay, TLC plates were blocked in 2.5% BSA (>98% fatty acid free; Sigma-Aldrich) in PBS for 2 h at room temperature. 2xFYVE-GST (250 ng/ml) was added to the blocking buffer for an additional 2 h. Plates were extensively washed with PBS and incubated with anti-GST (1 in 5000) in 1% BSA for 1 h. After washes with PBS, the plates were incubated with the HRP-labeled secondary antibodies for 1 h in 1% BSA, washed in PBS, and signals were detected by SuperSignal West Pico (Pierce Chemical, Rockford, IL).

Image Analysis of 2xFYVE-Enhanced Green Fluorescent Protein (EGFP) Vesicular Staining during Wortmannin Treatment

To analyze changes in fluorescence intensity of 2xFYVE-positive vesicles and cytosol before and after wortmannin treatment (15–20 min), three or more fluorescent vesicular structures and cytosolic regions were selected (avoiding puncta disappearing out of the optical section in the time lapse), and a region of interest outlined to measure their fluorescence intensity over time by using the LSM 510 software. The loss in 2xFYVE-positive organelles staining after wortmannin treatment was calculated based on the percentage change in the ratio of the organelles' fluorescence over cytosolic fluorescence.

Time-Lapse Confocal Microscopy Imaging

Confocal microscope (LSM 510 Meta; Carl Zeiss) laser power was set <4% for 488 nM argon laser and <20% for 543 nM HeNe laser; pinhole was 173 μm and optical section generally was kept at 1 μm by using a 63× water immersion objective (numerical aperture = 0.93). The pinhole was chosen to give rise to 1.7-μm confocal *z*-sections. The frequency of acquisition was two frames per minute over the incubation period indicated in the figure. Nicotine (100 μM) was applied by injection using a Hamilton syringe as indicated in the figures.

Four-Dimensional (4D) Confocal Analysis of 2xFYVE-EGFP Staining during Nicotine Treatment

Labeled organelles that remained in the same optical section throughout the duration of imaging were selected for intensity analysis. The changes in intensity of 2xFYVE-EGFP fluorescence from regions of interest in the cytosol and identified organelles were followed over time before and after nicotine treatment as described in the previous section but using maximum projection of *z*-stacks. The values were recorded and expressed as percentage increase of the normalized initial fluorescence intensity of 2xFYVE-EGFP.

Calcium Sensor Fluo-4/Acetoxymethyl Ester (AM) Experiment

PC12 cells were transfected with 2xFYVE-cherry for 15–24 h before use in experiment. Cells were briefly washed with Hanks' balanced salt solution (HBSS): 137 mM NaCl, 5.4 mM KCl, 0.25 mM Na_2HPO_4, 0.44 mM KH_2PO_4, 1.3 mM $CaCl_2$, 1 mM $MgSO_4$, and 4.2 mM $NaHCO_3$, pH 7.4, before being loaded with 2 μM Fluo-4/AM (Invitrogen) plus 1 μM Pluronic acid for 45 min at room temperature in HBSS. Dye-loaded cells were washed with HBSS for an additional 30 min at room temperature, and changes in fluorescence intensity were monitored by confocal microscopy.

Time-Lapse Confocal Microscopy Imaging of Digitonin-permeabilized Cells

Transfection of chromaffin cells were performed with an Amaxa Rat Neuron Nucleofactor kit (Quantum Scientific, Murarrie, QLD, Australia) according to the manufacturer's instructions. After 48–72 h, cells were washed with the indicated KGEP buffer and visualized by confocal microscopy. For time-lapse movies, cells were captured at 3 s/frame over 7-min periods. Cells were digitonin (2.5 μM)-permabilized in KGEP buffer containing Mg-ATP in the presence or absence of free Ca^{2+}. The image analysis was performed as described above. Values were expressed as the ratios of the peak fluorescence intensity over the initial fluorescence intensity.

Immunoelectron Microscopy

Chromaffin cells were fixed in 8% paraformaldehyde/0.1% glutaraldehyde in PBS and then processed for frozen sectioning. Processing, sectioning, and labeling for PtdIns(3)P with the 2xFYVE-GST was carried out as described previously (Gillooly *et al*., 2000). Wild-type yeast or yeast strains lacking Vps34 were labeled in parallel to determine the specificity of the labeling for PtdIns(3)P, as in a previous study (Gillooly *et al*., 2000).

Knockdown of PI3K-C2α by Small Interfering RNA (siRNA) in PC12 Cells

Two independent PI3K-C2α double-stranded siRNA (805, 807) clones (Ambion, Austin, TX) were used. The sequence of the forward oligonucleotide for clone 805 is 5′-CCUGCUGUUCAAAGAAGCCtt-3′. The complementary sequence for clone 805 is 5′-GGCUUCUUUGAACAGCAGGtc-3′. The sequence of the forward oligonucleotide for clone 807 is 5′-GGAGGUUCUACAGAAUAAUtt-3′. The complementary sequence for clone 807 is 5′-AUUAUUCUGUAGAACCUCCtc-3′. The negative control Silencer siRNA (provided by the manufacturer) composed of a 19-base pair scrambled sequences with 3′dT overhangs. Dried oligonucleotides were resuspended in nuclease-free water and stored at −20°C ready for use. PC12 cells were transfected twice 24 and 48 h after plating of cells with siRNA805 (20 nM), siRNA807 (20 nM), or negative control siRNA (20 nM) using Lipofectamine-LTX (Invitrogen). Forty-eight hours after the second transfection, 2xFYVE-EGFP was coexpressed in PC12 cells and examined after 15–24 h. Knockdown efficiency was analyzed by Western blot using antibodies against PI3K-C2α and β-actin (Sigma-Aldrich) as loading control.

Subcloning of the 2xFYVE in PmCherry Vector

PmCherry C1 vector (kindly provided by R. Tsien, University of California, San Diego, CA) and 2xFYVE-EGFP were both digested using Nhe1/BSrG1. Pmcherry insert was ligated in with 2xFYVE-C2 vector by using DNA ligase (Roche Products).

Chromaffin Granule Recruitment Assays

Purified chromaffin granules were prepared from bovine adrenal medulla as described previously (Bon *et al*., 1990; Vitale *et al*., 1996; Meunier *et al*., 2005; Osborne *et al*., 2007). We incubated 125 μg of granules per assay with 0.5 μg of 2xFYVE-GST for 30 min at 37°C in KGEP buffer containing 2 mM free Mg^{2+} and 2 mM ATP and the indicated concentrations of free calcium calculated using the WEBMAXC program (Patton *et al*., 2004). Reactions were stopped by diluting with 750 μl of ice-cold KGEP buffer and chromaffin granules isolated by centrifugation for 45 min at 100,000 × g_{av} (TLA100.4). Pellets were resuspended in Laemmli sample buffer containing β-mercaptoethanol and heated for 3 min at 95°C before separation by SDS-polyacrylamide gel electrophoresis (PAGE) and analysis by Western blotting with anti-GST antibodies (Sigma-Aldrich).

Analysis of Phosphoinositide Kinase Activity

HEK293 cells were transiently transfected with a cDNA construct encoding EE-tagged PI3K-C2α-pcDNA3.1 by using calcium phosphate. After 2 d, cultures were lysed with 10 mM Tris-HCl, pH 7.6, 5 mM EDTA, 50 mM NaCl, 30 mM sodium pyrophosphate, 50 mM NaF, 100 μM Na_3VO_4, 1% Triton X-100, and 1 mM phenylmethylsulfonyl fluoride (lysis buffer) and clarified by centrifugation at 4°C (14,000× *g* for 20 min). Recombinant enzyme was isolated by immunoprecipitation using anti-PI3K-C2α antisera and protein A-Sepharose. Immune complexes were washed with lysis buffer and twice with 139 mM potassium glutamate, 5 mM EGTA, and 20 mM PIPES, pH 6.8 (KGEP buffer). Recombinant enzyme was then aliquoted and incubated at 4°C with KGEP buffer, pH 7.4, containing 2 mM ATP, 2 mM $MgCl_2$, 10 μg of PtdIns, and varying concentrations of $CaCl_2$. After addition of radiolabeled [γ^{32}P]ATP (2 μCi) samples were incubated for 30 min at room temperature. Reactions were terminated by addition of 200 μl of 1 M HCl and phosphoinositides were extracted with 400 μl of chloroform:methanol (1:1, vol/vol). Reaction products were fractionated by TLC by using oxylate pretreated Silica Gel 60 plates and a 4 M NH_4OH:chloroform:methanol (11:50:39) solvent system. Radiolabeled PtdIns(3)P was quantified using a PhosphorImager (GE Healthcare, Little Chalfont, Buckinghamshire, United Kingdom), and data are expressed as phosphorimager units.

Statistical Analysis

Data analysis was carried out using Student's *t* test. Experiments were performed at least three times. Values are expressed as mean ± SEM, and data are considered significant at *$p < 0.05$, **$p < 0.01$.

RESULTS

Identification of an Additional Pool of PtdIns(3)P on LDCVs in Neurosecretory Cells

In view of the recent role found for class II PI3K-C2α in promoting exocytosis and its localization on mature secretory granules in chromaffin cells, we hypothesized that, in these cells, two pools of PtdIns(3)P might coexist and be synthesized on different organelles by distinct enzymes: class III PI3K (hvps34p) on early endosomes and class II PI3K-C2α on secretory vesicles. To visualize the pool of PtdIns(3)P-positive organelles in neurosecretory cells, GST-tagged 2xFYVE^{Hrs} domain (Gillooly *et al*., 2000) was used (referred to from hereon as 2xFYVE). The PtdIns(3)P-specific 2xFYVE domain was bacterially expressed as a GST fusion protein (2xFYVE-GST), and its ability to probe for PtdIns(3)P-positive organelles was positively verified in yeast by electron microscopy (data not shown) as described previously (Gillooly *et al*., 2000). We next investigated the ultrastructural localization of the 2xFYVE-GST staining in chromaffin cells by immunoelectron microscopy. Immunogold particles could be detected in the lumen of late endosomes (Figure 1A) as described previously (Gillooly *et al*., 2000). Importantly, in chromaffin cells, the membrane of some LDCVs were also immunogold positive (Figure 1A), demonstrating that a subpopulation of LDCVs can indeed be producing PtdIns(3)P.

To confirm this result, immunocytochemistry analysis of 2xFYVE-positive organelles was performed on chromaffin cells. The cells were preincubated with wortmannin (100 nM) for 20 min to eliminate early endosomal staining and digitonin-permeabilized in the presence of 2xFYVE-GST for 10 min. After washing and fixation, the 2xFYVE-positive organelles were revealed with an anti-GST antibody and costained with an anti-synaptotagmin 1 (Syt1) antibody, a marker for secretory granules. A clear colocalization pattern was observed demonstrating that Syt1-positive vesicles were also positive for 2xFYVE staining (Figure 1B and Supplemental Movie 1). Image analysis shows that the percentage of colocalization between the 2xFYVE-positive vesicles and Syt1 significantly increases in the presence of wortmannin (100 nM) from 34 ± 4 to 77 ± 5% in chromaffin cells and from 43 ± 3 to 71 ± 2% for PC12 cells. Furthermore, mature secretory granules were also found to be PtdIns(3)P-positive as revealed by a clear level of colocalization between P18, a processed cleavage product of secretogranin 2 (Wendler *et al*., 2001) and the 2xFYVE-GST staining (Supplemental Figure 1). We next expressed an EGFP-tagged version of the 2xFYVE probe in various cellular settings and exposed these cells to several pharmacological or genetic manipulations. 2xFYVE-EGFP expression in HEK293 cells or PC12 cells exhibited a vesicular punctate staining pattern, as described previously (Gillooly *et al*., 2000). Application of wortmannin (100 nM) caused the elimination of 2xFYVE-EGFP staining on organelles in HEK293 cells (Figure 2A and Supplemental Movie 2) likely to result from the inhibition of the wortmannin-sensitive class III PI3K in good agreement with a previous study (Pattni *et al*., 2001). Analysis of the fluorescence intensity of 2xFYVE-EGFP–positive identified organelles after wortmannin treatment revealed a complete loss of 2xFYVE-EGFP staining with a half-time of 1.9 ± 0.3 min (Figure 2G and Table 1). Examination of the fluorescence intensity of 2xFYVE-EGFP–positive organelles in PC12 cells treated with wortmannin (100 nM) revealed two populations of organelles with differential sensitivities to wortmannin (Figure 2B, Table 1, and Supplemental Movie 3). As described in HEK cells, a population of PtdIns(3)P-positive organelles from PC12 cells were sensitive to wortmannin inhibition (Figure 2B). Notably, a subpopulation of PtdIns(3)P-positive organelles were not affected by this concentration of wortmannin (Figure 2B and Supplemental Movie 3). We next tested whether the wortmannin-insensitive PtdIns(3)P pool could be eliminated by higher wortmannin concentration (1 μM). Such treatment resulted in a complete disappearance of the 2xFYVE-EGFP staining from all visible organelles (Table 1 and Supplemental Movie 4). Control experiments from untreated 2xFYVE-EGFP expressing PC12 cells showed no overall change in the intensity of

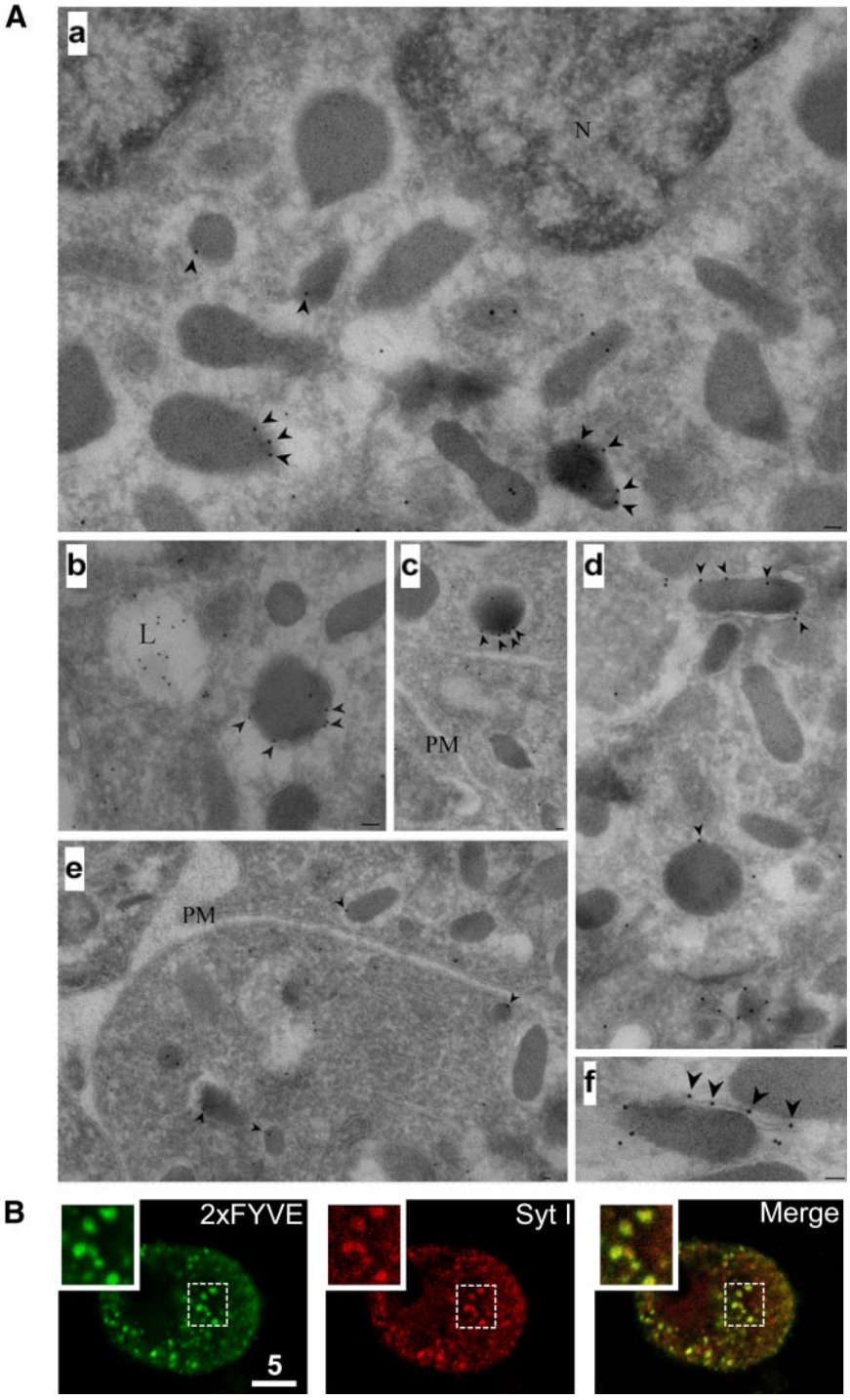

Figure 1. PtdIns(3)P-positive secretory granules in chromaffin cells revealed using 2xFYVE-GST by immunocytochemistry and immunoelectron microscopy. (A) Ultrathin frozen sections of cultured bovine chromaffin were labeled with 2xFYVE-GST and then with anti-GST and protein A-gold 10 nm to localize PtdIns(3)*P*. a–c show low-magnification overviews. Labeling is apparent in putative late endosomes (L) and associated with the cytoplasmic surface of electron dense granules (arrowheads). Labeling is variable with some granules showing particularly high labeling (e.g., b, c, d, and f). Note the labeling of a tubular element associated with the granule surface in d. As in other cells, the plasma membrane (PM) shows negligible labeling (e). (B) Wortmannin-treated (100 nM) chromaffin cells (20 min) were digitonin-permeabilized (20 μM), in KGEP buffer in the presence of 2xFYVE-GST (6.8 μM) for 10 min, briefly washed in KGEP buffer and fixed with 4% PFA. Cells were processed for immunocytochemistry by using anti-GST (left) and anti-Syt1 (right) antibodies. Cells were examined using confocal microscopy.

individual organelles during the time of experiment (Table 1 and Supplemental Movie 5).

The Newly Identified PtdIns(3)P Pool Is Produced by Class II PI3K-C2α in Neurosecretory Cells

Our experiments suggest that more than one type of PI3K may be operating on PtdIns(3)P-positive organelles in neurosecretory cells. In PC12 cells, like in HEK cells, wortmannin (100 nM) is likely to inhibit the synthesis of PtdIns(3)P produced by hvps34p that is located on the early or late endosomes (Christoforidis *et al.*, 1999; Stein *et al.*, 2003). PI3K-C2α is unique among all other types of PI3K in that it has a much reduced sensitivity to the classical PI3K inhibitor wortmannin ($IC_{50} \sim 420$ nM) (Domin *et al.*, 1997; Vanhaesebroeck *et al.*, 2001) and therefore could be responsible for the wortmannin-insensitive pool of PtdIns(3)P detected on a vesicular compartment in our experiments. Because PI3K-C2α has recently been localized on LDCVs in neurosecretory cells (Meunier *et al.*, 2005), our experiments indicated that wortmannin-insensitive PtdIns(3)P production could be mediated by PI3K-C2α on the LDCVs. To investigate this, a knockdown strategy by RNA interference was used. Control

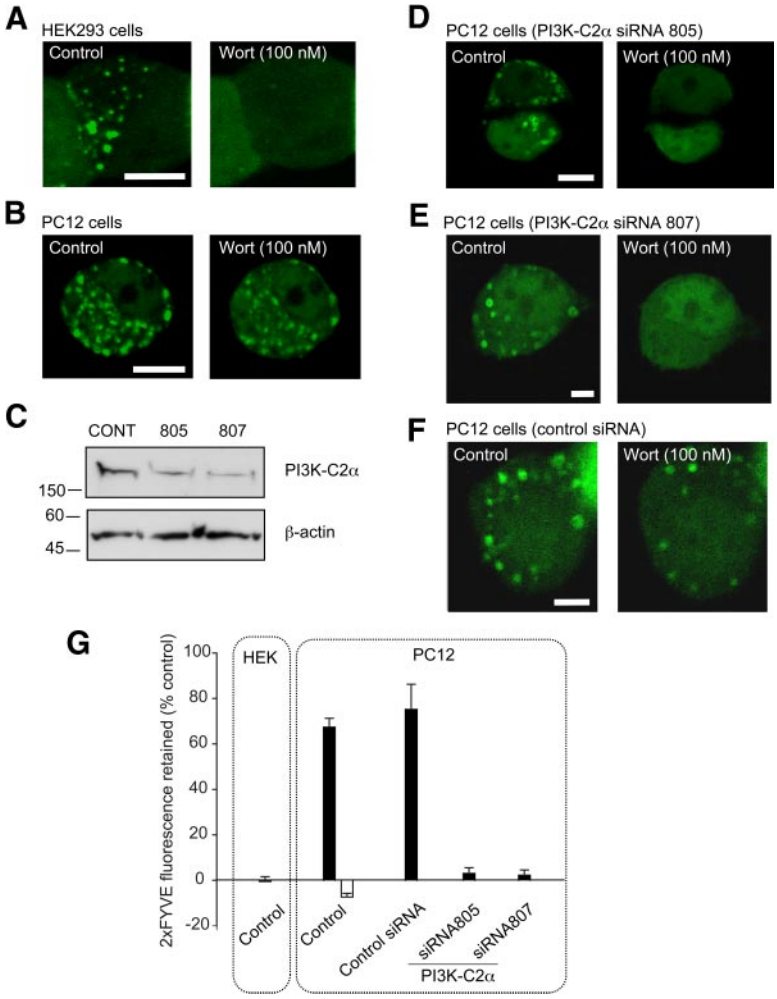

Figure 2. Wortmannin-insensitive vesicular PtdIns(3)P pool is abolished by PI3K-C2α knockdown in PC12 cells. HEK293 cells (A) or PC12 cells (B, D, E, and F) were transfected with 2xFYVE-EGFP for 15–24 h before live-cell imaging. In the knockdown experiments (D–F), PC12 cells were pretransfected (48 h earlier) with PI3K-C2α siRNA (805, 807) (D and E) or control siRNA (F). Cells were imaged at two frames/min in buffer A in the presence of (100 nM) wortmannin (A, B, D, E, and F). The image on the left and right represent the cells imaged before and after wortmannin treatment. (C) PC12 cells were transfected with either control siRNA or two different PI3K-C2α siRNA were lysed and probed for PI3K-C2α expression by Western blot by using an anti-PI3K-C2α. Anti-β-actin was used as loading control. (G) Quantification of the percentage of 2xFYVE-EGFP fluorescence retained on vesicles after wortmannin treatment. Black bar (100 nM), white bar (1 μM). Data are representative of three to seven independent experiments and expressed as mean $\pm$ SEM (Student's t test, $p < 0.05$). Bar, 10 μm.

and two independent siRNA directed against PI3K-C2α were transfected in PC12 cells. Western blotting analysis shows that the levels of knockdown ranged between 60 and 75% (Figure 2C). siRNA-treated PC12 cells were cotransfected with 2xFYVE-EGFP and treated with wortmannin (100 nM). The PI3K-C2α knockdown cells using both siRNA completely lost their 2xFYVE-EGFP–positive organelle staining upon wortmannin (100 nM) treatment (Figure 2, D, E, and G). In view of the apparent discrepancy between the knockdown levels (Figure 2C) and the wortmannin sensitivity of the PtdIns(3)P production (Figure 2G), it is worth noting that the latter experiment was based on a limited number of PC12 cells taken from a cell population where 83 $\pm$ 4% (203–222 cells examined) of the cells showed a significant knockdown as determined by PI3K-C2α immunostaining (Supplemental Figure 2). Alternatively, an incomplete PI3K-C2α knockdown at a single-cell level might be sufficient to fully perturb the wortmannin sensitivity of the PC12 cell. Importantly, control siRNA-treated cells retained significant amount of vesicular 2xFYVE-EGFP staining upon wortmannin treatment (Figure 2, F and G).

Table 1. Wortmannin sensitivity of 2x FYVE-EGFP–positive organelles

Cell type and conditions	Time constant (min)	Half-time (min)	Intensity change (%)
PC12 cells			
Control (n = 31, 5 cells)	>20	>20	−3 ± 9
Wortmannin (100 nM)			
WISO (n = 23, 7 cells)	>20	>20	4 ± 6
WSO (n = 27, 7 cells)	7.2 ± 0.5	4.9 ± 0.3	78.30 ± 4
Wortmannin (1 μM) (n = 43, 6 cells)	1.7 ± 0.4	1.2 ± 0.3	107.3 ± 2
HEK293 cells			
Wortmannin (100 nM) (n = 37, 6 cells)	2.7 ± 0.5	1.8 ± 0.3	100.5 ± 2.1

WISO, wortmannin-insensitive organelles; WSO, wortmannin-sensitive organelles.

PtdIns(3)P Synthesis Transiently Increase on LDCVs in Response to Stimulation

Having demonstrated that PI3K-C2α was indeed responsible for the production of PtdIns(3)P on a population of secretory vesicles in neurosecretory cells, we investigated whether stimulation of exocytosis would alter PtdIns(3)P levels on identified vesicles. Lifetime 4D imaging of 2xFYVE-EGFP–expressing PC12 cells was carried out using confocal microscopy (Supplemental Movie 6). Three-dimensional (3D) z-stacks were taken before and during the addi-

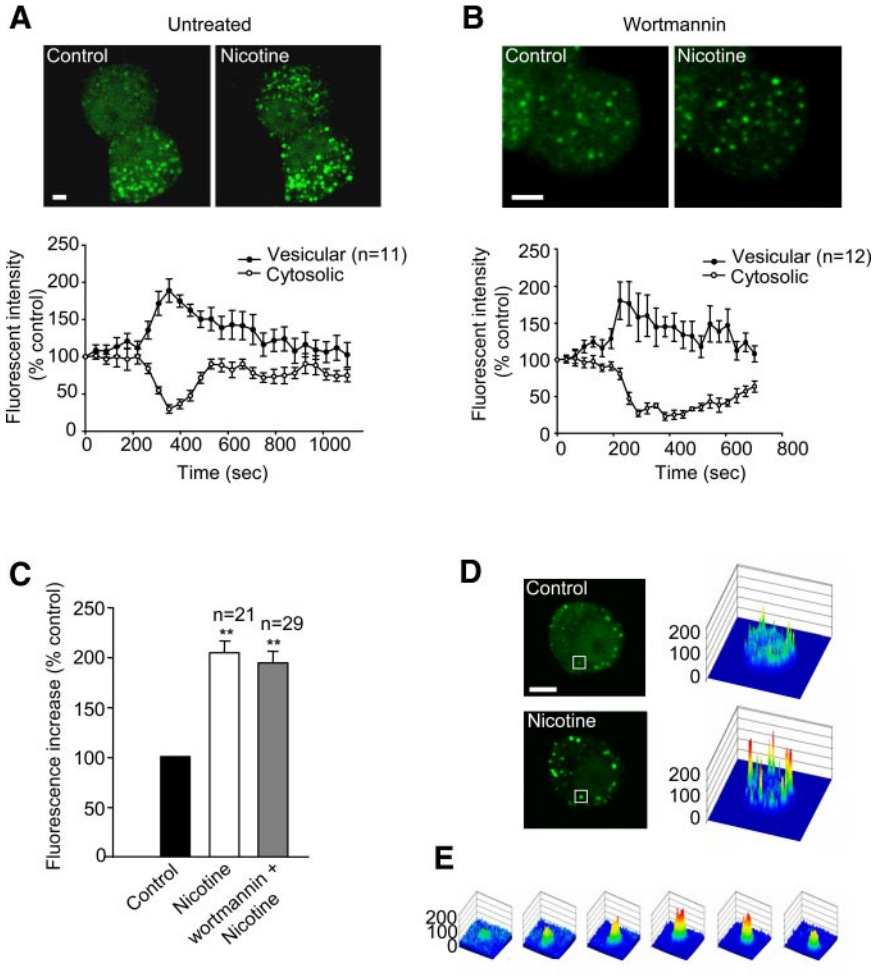

Figure 3. Stimulation of exocytosis by nicotine promotes a transient recruitment of 2xFYVE onto vesicles in PC12 cells. PC12 cells were transfected with 2xFYVE-EGFP for 15–24 h before live-cell imaging. Cells were pretreated with buffer A containing 2 mM $CaCl_2$ in the absence (A and D) or presence (B) of wortmannin (50 nM) for 25–30 min. Control (A and D) or wortmannin pretreated (B) cells were then examined by time-lapse confocal microscopy at two frames/min. Initial 4D movie was used to obtain a 3D projection image (A) before (left) and after (right) nicotine (100 μM) treatment. Time course of the changes in 2xFYVE-EGFP vesicular and cytosolic fluorescence intensities were analyzed (A and B, bottom). (C) Bar graphs show the variation of vesicular fluorescence intensity at the peak of nicotine action. (D) Surface plot analysis (right) of changes in fluorescence intensity after nicotine stimulation in a 2xFYVE-EGFP–transfected PC12 cell before and at the peak of nicotine action. (E) Surface plot analysis of an identified vesicle identified in a square in D during nicotine treatment. Data shown are representative of four to six independent experiments. The numbers of vesicles and cytosolic measurements are expressed as mean ± SEM (Student's *t* test, $^{**}p < 0.01$). Bar, 5 μm.

tion of nicotine—a well-characterized secretagogue for PC12 cells. Figure 3A shows a 3D-maximum projection taken before and after nicotine stimulation. The vesicular fluorescence intensity increased dramatically, whereas that of the cytosol decreased concomitantly (Figure 3, A and D). This results suggest that upon nicotine stimulation, PtdIns(3)P production increased on a vesicular compartment which, in turn, act as a recruitment factor for the cytosolic 2xFYVE-EGFP. A similar experiment was carried out on PC12 cells previously pretreated with wortmannin to eliminate the early endosomal PtdIns(3)P production (Figure 3B). Similar 2xFYVE-EGFP recruitment was detected upon nicotine stimulation and analysis of the peak intensity revealed a doubling of the fluorescence intensity in the presence (93 ± 11%) or the absence (104 ± 10%) of wortmannin (Figure 3C). The increase in fluorescence on an identified secretory vesicle is depicted on Figure 3E. Similar results were obtained when using other secretagogues such as high potassium (data not shown). The PtdIns(3)P-binding deficient 2xFYVE[C215S]-EGFP mutant was used as a control, and no recruitment of the mutated probe could be detected upon nicotine stimulation of PC12 cells (data not shown). Our results suggested that the observed 2xFYVE recruitment could result from the intracellular Ca^{2+} rise known to occur upon such stimulation of exocytosis. To investigate this issue, 2xFYVE-Cherry expressing PC12 cells were loaded with the Ca^{2+}-sensing probe Fluo-4/AM. After nicotine addition, the rise in intracellular Ca^{2+} fluorescence was accompanied by 2xFYVE recruitment (Supplemental Figure 3). Importantly, both show similar kinetics, suggesting that these effects could be linked and that Ca^{2+} could initiate PtdIns(3)P production on LDCVs. To pursue this hypothesis, 2xFYVE-expressing cells were imaged before and during digitonin permeabilization in the presence of Ca^{2+}-containing buffers (Supplemental Figure 4). Importantly, a Ca^{2+}-dependent recruitment of the 2xFYVE domain could indeed be detected following Ca^{2+} entry (Supplemental Figure 4B).

We then turned to an in vitro analytical method to confirm our results using purified chromaffin granules. The purity of our preparation was established previously (Bon *et al.*, 1990; Vitale *et al.*, 1996; Meunier *et al.*, 2005; Osborne *et al.*, 2007), and Western blot analysis demonstrated that no early endosomal contamination could be detected (Meunier *et al.*, 2005). Chromaffin granules were first incubated in various conditions including ATP, cytosol extract. After lipid extraction and separation on TLC, PtdIns(3)P production was revealed by overlay assay using 2xFYVE-GST, anti-GST, and HRP-conjugated secondary antibodies sequentially. We confirmed that PtdIns(3)P was specifically synthesized on secretory granules and found that this production was facilitated in the presence of cytosol suggesting that a fraction of PtdIns(3)P could be regulated by cytosolic factors (Figure 4A). We next tested the Ca^{2+} dependency of PtdIns(3)P production by classical TLC analysis using [^{32}P]ATP and showed that a monophosphorylated phosphoinositide was produced on chromaffin granules and a clear enhanced synthesis was detected by

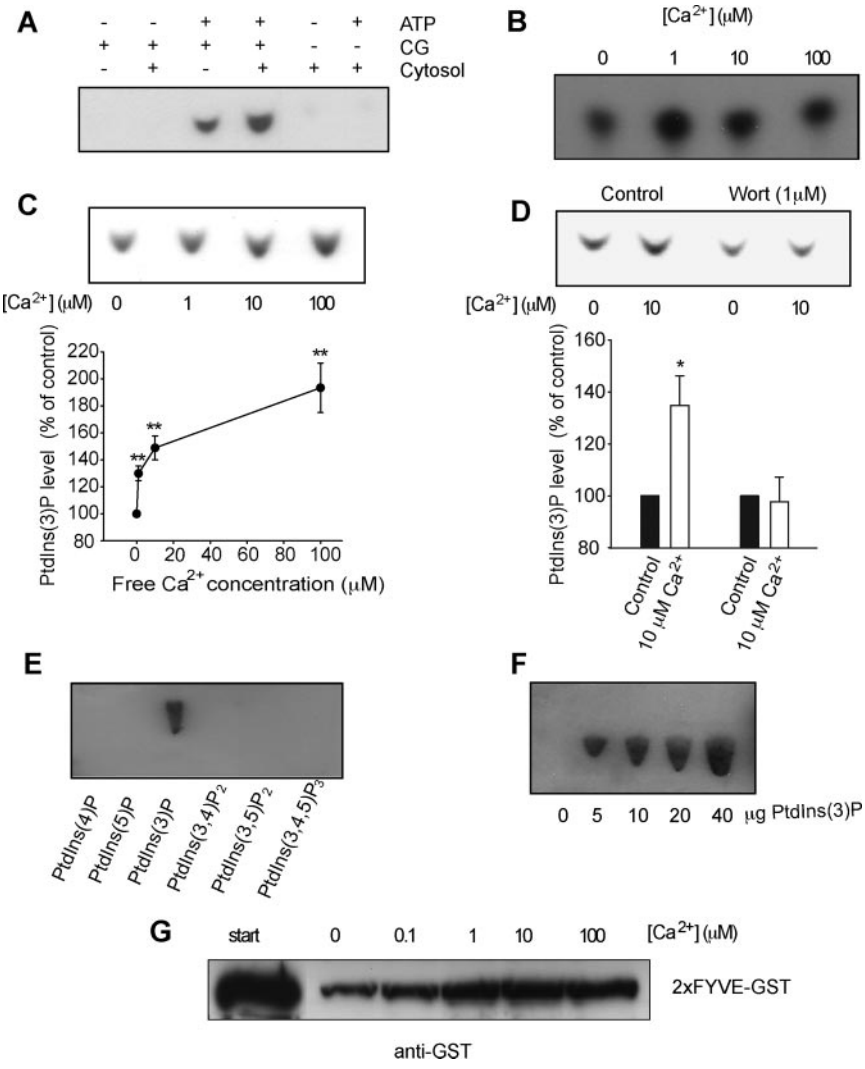

Figure 4. Ca^{2+}-dependent PtdIns(3)P production on purified chromaffin granules. (A) Purified chromaffin granules were incubated in the presence or absence of Mg-ATP and presence or absence of 500 μg of bovine adrenal medulla cytosol, phosphoinositides were extracted using acidified chloroform:methanol extraction and separated on oxalate treated TLC plates. PtdIns(3)P was visualized by incubating TLC plates consecutively with GST-2xFYVE domain, anti-GST antibodies, and HRP-labeled secondary antibodies and developing with SuperSignal West Pico. (B) Purified chromaffin granules were incubated with [^{32}P]ATP and varying amounts of free calcium as indicated. Labeled phosphoinositides were extracted and separated as in A. Spots were identified compared with unlabeled standards visualized using copper molybdate spray reagent. (C) Purified chromaffin granules were incubated in varying amount of free calcium in the presence of 500 μg of cytosol. Phosphoinositides were extracted, separated, and the amount of PtdIns(3)P probed by overlay using the GST-2xFYVE as described in A. The quantification of the increase in PtdIns(3)P level is shown in the graph (n = 3–8 experiments per condition). (D) Purified chromaffin granules incubated as in C with Mg-ATP, cytosol, and in the presence or absence of free Ca^{2+} (10 μM) and wortmannin (1 μM) before analysis of phosphoinositides as described in A. The Ca^{2+}-dependent increase in PtdIns(3)P production is blocked by wortmannin treatment as indicated in the graph (n = 4 control; n = 5 wortmannin). (E) Twenty micrograms of the synthetic lipids PtdIns(4)P, PtdIns(5)P, PtdIns(3)P, PtdIns(3,5)P_2, PtdIns(3,4)P_2, and PtdIns(3,4,5)P_3 (diC16, acid form) were spotted and separated on TLC plates and probed by overlay using the GST-2xFYVE as described in A. (F) Increasing amount of synthetic PtdIns(3)P spotted on the TLC plates as indicated on the figure was probed and overlaid by using the GST-2xFYVE as described in A. (G) Purified chromaffin granules were incubated with GST-2xFYVE domain in the presence of Mg-ATP and increasing concentrations of Ca^{2+}. Granules were isolated by centrifugation and associated GST-2xFYVE was visualized by SDS-PAGE and Western blotting using anti-GST antibodies.

increasing free Ca^{2+} concentration (Figure 4B). The nature of the monophosphorylated PtdIns up-regulated by Ca^{2+} was further investigated by overlay assay and confirmed to be PtdIns(3)P (Figure 4C). A significant Ca^{2+}-dependent increase in PtdIns(3)P production was detected as quantified in Figure 4C. Importantly, this Ca^{2+}-dependent PtdIns(3)P synthesis was sensitive to wortmannin pretreatment of the secretory granules (Figure 4D). The specificity of the 2xFYVE domain to PtdIns(3)P in our overlay assay was confirmed by undetectable binding of the probe to PtdIns(4)P, PtdIns(5)P, PtdIns(3,4)P_2, PtdIns(3,5)P_2, and PtdIns(3,4,5)P_3 (Figure 4E). Furthermore, the dynamic range of the 2xFYVE binding to PtdIns(3)P is shown in Figure 4F. Finally, we checked that 2xFYVE-GST was recruited on isolated chromaffin granules in a Ca^{2+}-dependent manner using a binding assay on intact purified granules. Purified granules were incubated with 2xFYVE-GST in increasing concentrations of free Ca^{2+}. The granules were recovered by centrifugation and the amount of 2xFYVE-GST domain associated with the granules was analyzed by SDS-PAGE and Western blotting using an anti-GST. A clear Ca^{2+}-dependent recruitment of the 2xFYVE-GST was observed (Figure 4G).

The Activity of Class II PI3K-C2α Is Regulated by Ca^{2+}

Although PI3K are highly regulated proteins, to the best of our knowledge, no Ca^{2+} dependency in their kinase activity has been reported so far. PI3K-C2α activity was known to occur in the presence of Ca^{2+} (Arcaro *et al.*, 2000), we therefore tested whether it was directly up-regulated by Ca^{2+}. Recombinant PI3K-C2α was expressed in HEK cells and immunoprecipitated to carry out a kinase assay as described previously (Meunier *et al.*, 2005). Increasing the free Ca^{2+} concentration in the lipid kinase assay to 0.5 and 1 μM produced a 2.4- and 3.9-fold increase in PtdIns(3)P production over that obtained in the absence of Ca^{2+} (Figure 5). At higher concentrations, the activity returned to basal levels.

Class II PI3K-C2α Is Responsible for Ca^{2+}-dependent PtdIns(3)P Signaling Restricted on LDCVs in Neurosecretory Cells

We then investigated whether PI3K-C2α was mediating the Ca^{2+}-dependent PtdIns(3)P increase in PC12 cells. In view of the dominant-negative effect of PI3K-C2α [R1251P] kinase-

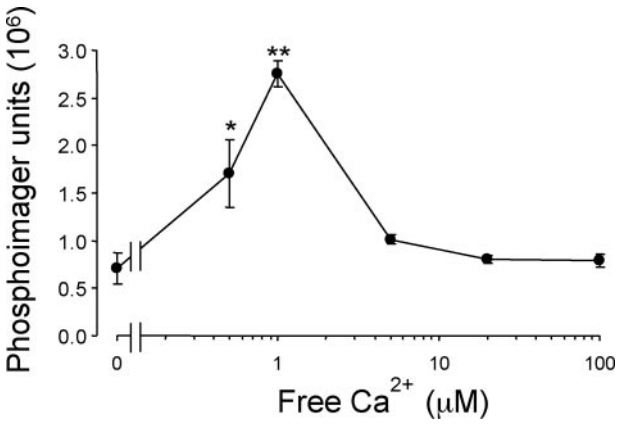

Figure 5. PI3K-C2α lipid kinase activity is regulated by micromolar concentrations of Ca^{2+}. Recombinant PI3K-C2α was expressed in HEK293 cells and immunoprecipitated with anti-PI3K-C2α antisera. Aliquots were incubated with PtdIns (10 μg) in KGEP buffer, pH 7.4, containing 2 mM ATP (2 μCi of [γ-^{32}P]ATP) and 2 mM $MgCl_2$. After 30 min at room temperature, phosphoinositides were extracted, fractionated by TLC, and PtdIns(3)P was quantified by PhosphorImager analysis. Data are expressed as phosphorimager units representing mean ± SEM (n = 3 independent experiments).

inactive mutant on exocytosis (Meunier *et al*., 2005), it was tempting to hypothesize that expression of PI3K-C2α [R1251P] could be responsible for preventing the Ca^{2+}-dependent production of PtdIns(3)P on secretory vesicles upon stimulation of exocytosis. We therefore coexpressed PI3K-C2α wild-type (wt) and 2xFYVE-Cherry in PC12 cells. Nicotine stimulation promoted a transient recruitment of the 2xFYVE domain on a vesicular compartment (Figure 6A) similar to that observed in Figure 3. Importantly this recruitment was blocked in PC12 cells overexpressing PI3K-C2α [R1251P], indicating that PI3K-C2α is indeed responsible for producing PtdIns(3)P in a Ca^{2+}-dependent manner (Figure 6, B and C). The specific requirement for PI3K-C2α activity in promoting this Ca^{2+}-dependent PtdIns(3)P synthesis on secretory granules was further investigated using siRNA knockdown of PI3K-C2α. Two independent siRNAs used to knock down PI3K-C2α prevented the nicotine-induced recruitment of 2xFYVE-EGFP in PC12 cells (Figure 7). The level of PI3K-C2α expression in control and two independent PI3K-C2α siRNAs was verified by immunocytochemistry in PC12 cells (Supplemental Figure 2).

DISCUSSION

PtdIns(4,5)P_2 has long been known to play a critical role in mediating exocytosis (Eberhard *et al*., 1990; Milosevic *et al*., 2005; Osborne *et al*., 2007; James *et al*., 2008). Distinct 3-phosphorylated phosphoinositides have been shown to both stimulate [PtdIns(3)P] and inhibit [PtdIns(3,5)P_2] exocytosis from neurosecretory cells (Meunier *et al*., 2005; Osborne *et al*., 2008).

In the present study, we have used PtdIns(3)P-selective domains combined with electron microscopy, real-time confocal imaging, immunocytochemistry and biochemistry to study the localization and dynamics of PtdIns(3)P in neurosecretory cells. Our findings reveal a pool of PtdIns(3)P

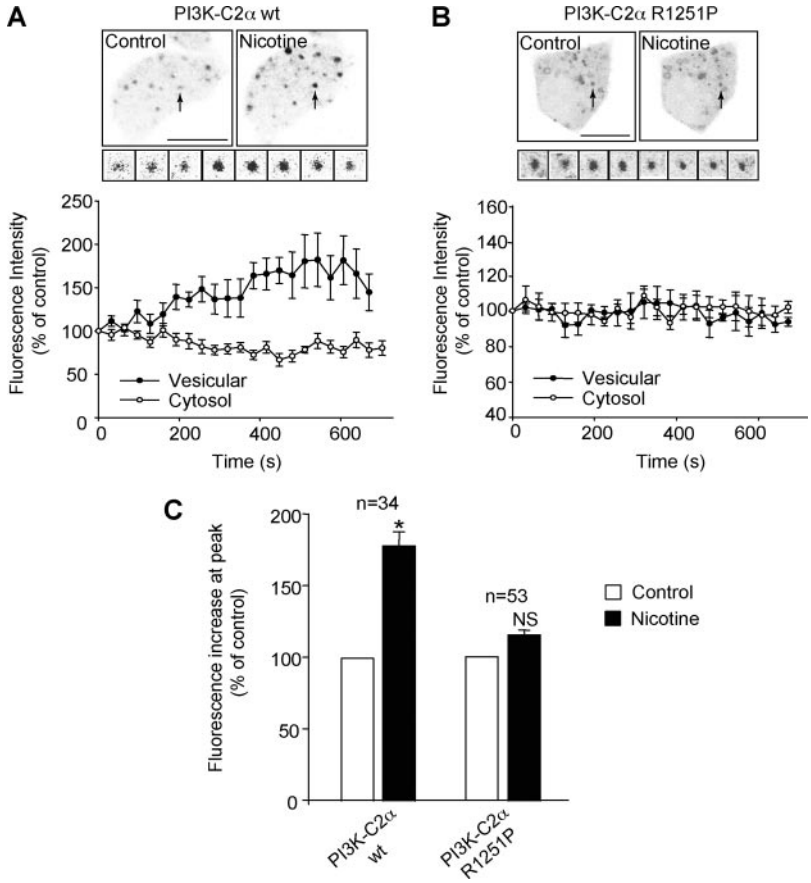

Figure 6. Expression of the catalytically inactive PI3K-C2α-R1251P but not the WT PI3K-C2α in PC12 cells severely abolished the recruitment of 2xFYVE onto vesicles upon nicotine stimulation. PC12 cells were cotransfected with either PI3K-C2α-wt (A) or PI3K-C2α-R1251P (B) and 2xFYVE-Cherry for 15–24 h before live-cell imaging. Images before and after nicotine stimulation are displayed in inverted black-and-white colors to show the change in vesicular intensity. The insets show the fluorescence intensity change of an identified 2xFYVE-positive vesicles upon nicotine stimulation. The time course of variation in vesicular (n = 5 for PI3K-C2α-wt; n = 6 for PI3K-C2α-R1251P) and cytosolic (n = 4) intensity is shown (A and B, bottom). (C) Bar graph shows the amplitude of 2xFYVE fluorescence increase at the peak of nicotine action (n = 5). Data are representative of eight to nine independent experiments. The measurements of the vesicular and cytosolic fluorescence intensities are expressed as mean ± SEM (Student's *t* test, *p < 0.05). Bar, 5 μm.

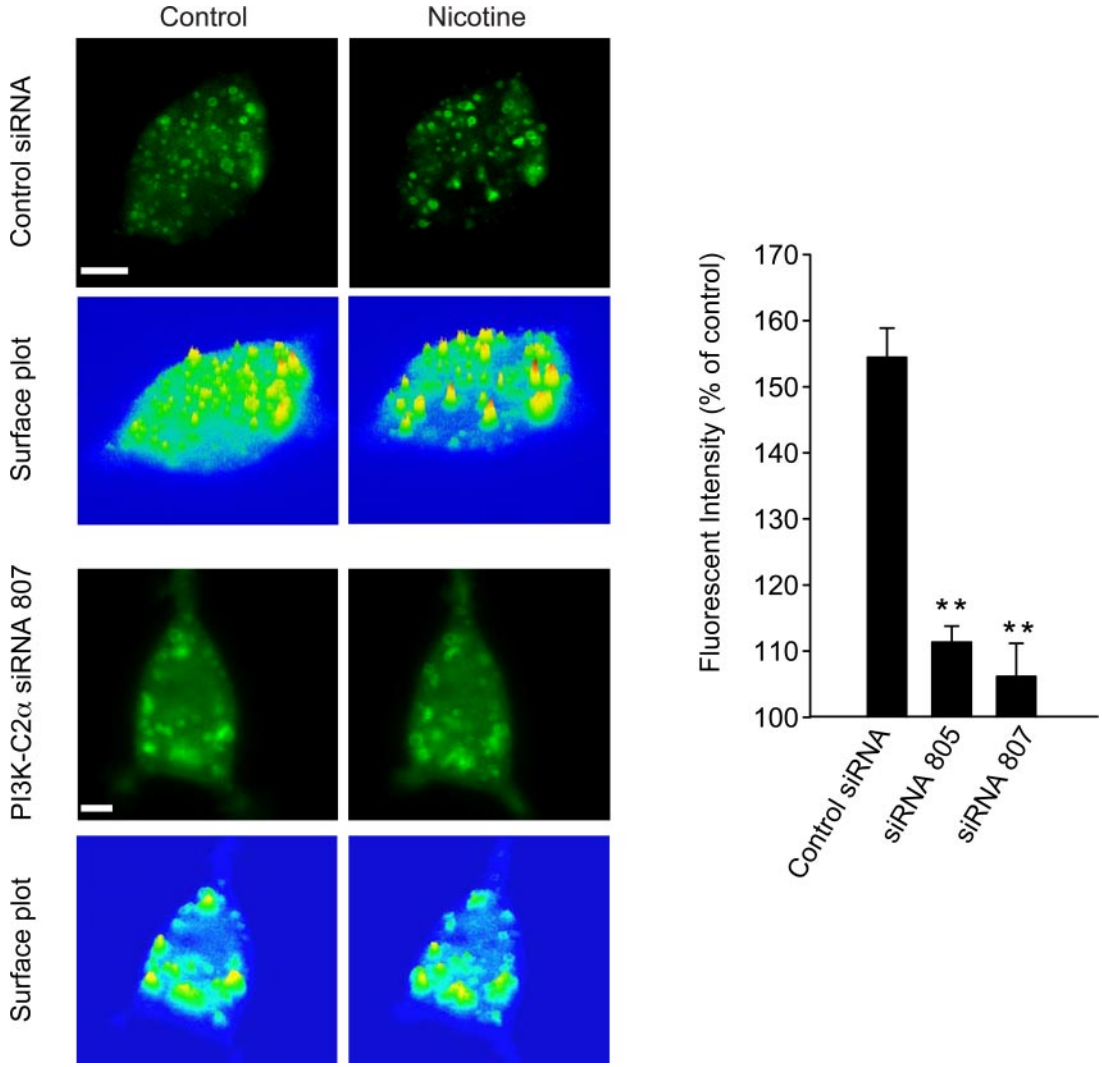

Figure 7. PI3K-C2α knockdown prevents the Ca^{2+}-dependent increase in PtdIns(3)P production on neurosecretory vesicles. PC12 cells were pretransfected (48 h earlier) with control siRNA or PI3K-C2α siRNA (805, 807) and transfected with 2xFYVE-EGFP for 15–24 h before live-cell imaging. Cells were examined by time-lapse confocal microscopy at two frames/min before (left) and after (right) nicotine (100 μM) treatment. Initial 4D movie was used to obtain a 3D projection image. Surface plot analysis of cells before and during nicotine treatment shows the change of fluorescence intensity of intracellular 2xFYVE-EGFP–positive vesicles (as indicated in the figure). Bar graphs show the variation of vesicular fluorescence intensity at the peak of nicotine action in the indicated experimental conditions. Data shown are representative of 4 independent experiments. The fluorescence intensity changes on identified vesicles (control siRNA, n = 11; siRNA 805, n = 21; siRNA 807, n = 27) are expressed as mean ± SEM (Student's *t* test, **$p < 0.01$). Bar, 5 μm.

produced by PI3K-C2α on LDCVs, which is up-regulated by Ca^{2+} during stimulation of exocytosis. Furthermore, our study reveals that Ca^{2+} directly regulates the kinase activity of a member of the PI3K family.

Distinct Pools of PtdIns(3)P in Neurosecretory Cells

The subcellular distribution of PtdIns(3)P has primarily been investigated using 2xFYVE domains in cells of non-neurosecretory origin (e.g., Madin-Darby canine kidney, normal rat kidney, HeLa) (Balla and Varnai, 2002; Hayakawa *et al.*, 2004) where it has been localized mainly to early endosomes (Gillooly *et al.*, 2000; Pattni *et al.*, 2001; Petiot *et al.*, 2003). The endosomal pool of PtdIns(3)P shows a high sensitivity to wortmannin treatment and has been largely attributed to the activity of class III PI3K (Gillooly *et al.*, 2000; Pattni *et al.*, 2001). In sharp contrast, in PC12 cells expressing 2xFYVE-EGFP domain, wortmannin treatment revealed two distinct pools of PtdIns(3)P-positive organelles distinguished by their sensitivity to wortmannin. Immunocytochemistry analysis showed that wortmannin-insensitive PtdIns(3)P-positive organelles were predominantly LDCVs as evidenced by their strong colocalization with synaptotagmin 1 and mature secretogranin P18. To our best knowledge, this is the first time that PtdIns(3)P has been shown to be present on LDCVs in neurosecretory cells.

Because PI3K-C2α is notoriously resistant to wortmannin (Domin *et al.*, 1997), it is highly likely that PI3K-C2α is responsible for the wortmannin-insensitive PtdIns(3)P production found in neurosecretory cells. The RNA interference knockdown of PI3K-C2α confirmed this view by revealing the disappearance of the wortmannin-insensitive pool of PtdIns(3)P (Figure 2). Our data demonstrate that in neurosecretory cells, PI3K-C2α produces PtdIns(3)P on LDCVs, whereas type III PI3K synthesizes PtdIns(3)P on early endo-

somes. It remains possible however that PI3K-C2α could act as a back-up mechanism to produce PtdIns(3)P also on some early endosomes as has been suggested recently (Johnson *et al.*, 2006). However, if true, this mechanism is unlikely to be significant in neurosecretory cells as PI3K-C2α was not detected on early endosomes (Christoforidis *et al.*, 1999; Meunier *et al.*, 2005).

PI3K-C2α Synthesizes PtdIns(3)P on LDCVs

Several lines of evidence suggests that PI3K-C2α synthesizes PtdIns(3)P on LDCVs in both PC12 cells and chromaffin cells. First, PI3K-C2α has been localized on LDCVs in chromaffin (Meunier *et al.*, 2005) and PC12 cells (data not shown). Second, PI3K-C2α knockdown abolishes the wortmannin insensitivity of PtdIns(3)P production in living PC12 cells (Figure 2). Third, 2xFYVE binding is clearly detected on chromaffin granules by immunoelectron microscopy, immunofluorescence (Figure 1) and in vitro (Figure 4). The reliance of 2xFYVE domain binding to PtdIns(3)P in most of our experiments warranted a careful examination of possible nonspecific 2xFYVE binding to other lipids. To eliminate this possibility, several overlay assays carried out in our study revealed that 2xFYVE does not interact with phosphatidic acid, phosphatidyl serine, phosphatidyl choline, phosphatidyl ethanolamine, and PtdIns (data not shown), in good agreement with another study (Gillooly *et al.*, 2000). The high selectivity of the 2xFYVE binding to PtdIns(3)P was further confirmed herein by using PtdIns(4)P, PtdIns(5)P, PtdIns(3,4)P_2, PtdIns(3,5)P_2, and PtdIns(3,4,5)P_3 (Figure 4E).

Previous work on chromaffin cells have localized PtdIns(4)P on LDCVs (Wiedemann *et al.*, 1996; Panaretou and Tooze, 2002). Our study therefore adds to the complexity of the phosphoinositide family members present on LDCVs and involved in the neurosecretory process (Meunier *et al.*, 2005; Osborne *et al.*, 2006). The data presented here suggest that neurosecretory cells have adapted an alternative mechanism requiring PtdIns(3)P synthesis on LDCVs that could potentially be used to recruit effector(s) involved in promoting ATP-dependent priming of LDCVs (Meunier *et al.*, 2005).

De Novo Synthesis of PtdIns(3)P Pool by PI3K-C2α upon Stimulation of Exocytosis

We provide evidence indicating that PI3K-C2α activity can be up-regulated on LDCVs upon stimulation of exocytosis. First, 2xFYVE recruitment onto LDCVs was shown to occur in response to nicotine stimulation (Figure 3 and Supplemental Movie 6) and direct Ca^{2+} stimulation in digitonin-permeabilized neurosecretory cells (Supplemental Figure 4). Additional experiments using other secretagogues such as barium (2 mM) and high potassium (60 mM) in the presence of external Ca^{2+} gave similar results (data not shown). In the absence of external Ca^{2+}, no recruitment could be observed (data not shown). Moreover, using PC12 cells loaded with the Ca^{2+} indicator Fluo-4, we found that the kinetic of the Ca^{2+} transient elicited by nicotine addition closely match that of the 2xFYVE recruitment (Supplemental Figure 3). Second, overexpression of the catalytically inactive mutant of PI3K-C2α and siRNA knockdown of PI3K-C2α inhibit the nicotine-induced 2xFYVE recruitment (Figures 6 and 7). The Ca^{2+}-dependent recruitment of the 2xFYVE domain could be mediated by alternative means such as protein–protein interactions and/or decreased PI3-phosphatase activity. However, our knockdown experiments and in vitro data using lipid extraction from purified chromaffin granules clearly indicate a specific Ca^{2+}-dependent PtdIns(3)P production mediated by PI3K-C2α (Figure 4, B–E). Finally, the most direct indication that the activity of PI3K-C2α is indeed regulated by Ca^{2+} comes from recombinantly expressed PI3K-C2α whose activity is demonstrated to be tightly controlled by Ca^{2+} (Figure 5). Future experiments are warranted to address the molecular basis of the Ca^{2+} dependency of PI3K-C2α activity. Notably, the Ca^{2+} dependency of PtdIns(3)P production on LDCVs and that of PI3K-C2α activity in vitro are only comparable up to 1 μM. For higher concentrations of Ca^{2+}, PI3K-C2α activity returns to basal level, whereas PtdIns(3)P production on LDCVs seems to plateau. This apparent discrepancy might be explained by the potentiating effect of cytosolic extract on PtdIns(3)P production from purified LDCVs (Figure 4A). Such cytosolic factors could help maintaining PI3K-C2α activity at higher Ca^{2+} concentrations known to occur in the vicinity of the plasma membrane upon activation of Ca^{2+} channels (Meunier *et al.*, 2002). This de novo synthesis of PtdIns(3)P on LDCVs further illustrates that PtdIns(3)P can be dynamically regulated in living cells beyond that previously reported in platelets (Zhang *et al.*, 1998), COS-7 cells (Razzini *et al.*, 2000), macrophages (Chua and Deretic, 2004), and L6 muscle cell line (Falasca *et al.*, 2007). Interestingly, one recent study has shown that Ca^{2+} can increase calmodulin binding to class III PI3K (Vergne *et al.*, 2003), supporting the idea that calmodulin could be involved in modulating PI3K-C2α on LDCVs in a Ca^{2+}-dependent manner. PI3K-C2α is also a key player in clathrin-mediated endocytosis and has recently been shown to link the cytoskeleton with clathrin (Gaidarov *et al.*, 2001, 2005; Zhao *et al.*, 2007). In this view, it would be interesting to see whether Ca^{2+} activation of PI3K-C2α provides with an extra layer of control in this process.

An interesting model is starting to emerge in which PI3K-C2α located on LDCVs is activated by Ca^{2+} and promotes the formation of PtdIns(3)P on neurosecretory vesicles. PtdIns(3)P can be converted to PtdIns(3,5)P_2 by PIKfyve, which has recently been shown to negatively regulate exocytosis (Osborne *et al.*, 2008). PIKfyve therefore provides a negative feedback regulation to avoid "overpriming," which could be detrimental to neurosecretory cells.

In conclusion, we found that in neurosecretory cells, a dynamic pool of PtdIns(3)P is synthesized by PI3K-C2α on LDCVs, revealing for the first time that the activity of a PI3K could be regulated by Ca^{2+}. Such an increase in PtdIns(3)P production on LDCVs upon stimulation of exocytosis could serve as a recruitment factor for effector(s) acting downstream of PI3K-C2α activity to promote ATP-dependent priming of LDCVs. Importantly, LDCV priming was originally found to be a Ca^{2+}-dependent process (Bittner and Holz, 1992) and the Ca^{2+} dependency of PI3K-C2α activity demonstrated herein may therefore contribute to this mechanism.

Further work will be required to 1) examine whether PtdIns(3)P-positive vesicles undergo an active translocation to the plasma membrane and 2) determine the nature of the priming effector(s). Novel prospective strategies coupling phosphoinositide pull down with mass spectrometry could help identify such effector(s) (Osborne *et al.*, 2007).

ACKNOWLEDGMENTS

We are indebted to Shawn Jackson and Simone Schoenwaelder (Australian Centre for Blood Diseases, Monash University) for insightful comments, preliminary experiments, and excellent suggestions; and G. Schiavo, S. Tooze, and Peter Parker (Cancer Research UK) for reagents, exciting discussions, and suggestions at an early stage of this work. This work was supported by a National Health and Medical Research Council (NHMRC) project grant (to F.A.M.). R.G.P. is a Principal Research Fellow of the NHMRC.

REFERENCES

Arcaro, A., Zvelebil, M. J., Wallasch, C., Ullrich, A., Waterfield, M. D., and Domin, J. (2000). Class II phosphoinositide 3-kinases are downstream targets of activated polypeptide growth factor receptors. Mol. Cell Biol. *20*, 3817–3830.

Balla, T., and Varnai, P. (2002). Visualizing cellular phosphoinositide pools with GFP-fused protein-modules. Sci. STKE *2002*, PL3.

Bittner, M. A., and Holz, R. W. (1992). Kinetic analysis of secretion from permeabilized adrenal chromaffin cells reveals distinct components. J. Biol. Chem. *267*, 16219–16225.

Bon, S., Bader, M. F., Aunis, D., Massoulie, J., and Henry, J. P. (1990). Subcellular distribution of acetylcholinesterase forms in chromaffin cells. Do chromaffin granules contain a specific secretory acetylcholinesterase? Eur. J. Biochem. *190*, 221–232.

Chasserot-Golaz, S., Hubert, P., Thierse, D., Dirrig, S., Vlahos, C. J., Aunis, D., and Bader, M. F. (1998). Possible involvement of phosphatidylinositol 3-kinase in regulated exocytosis: studies in chromaffin cells with inhibitor LY294002. J. Neurochem. *70*, 2347–2356.

Christoforidis, S., Miaczynska, M., Ashman, K., Wilm, M., Zhao, L., Yip, S. C., Waterfield, M. D., Backer, J. M., and Zerial, M. (1999). Phosphatidylinositol-3-OH kinases are Rab5 effectors. Nat. Cell Biol. *1*, 249–252.

Chua, J., and Deretic, V. (2004). Mycobacterium tuberculosis reprograms waves of phosphatidylinositol 3-phosphate on phagosomal organelles. J. Biol. Chem. *279*, 36982–36992.

Corvera, S., and Czech, M. P. (1998). Direct targets of phosphoinositide 3-kinase products in membrane traffic and signal transduction. Trends Cell Biol. *8*, 442–446.

Corvera, S., D'Arrigo, A., and Stenmark, H. (1999). Phosphoinositides in membrane traffic. Curr. Opin. Cell Biol. *11*, 460–465.

Cousin, M. A., Malladi, C. S., Tan, T. C., Raymond, C. R., Smillie, K. J., and Robinson, P. J. (2003). Synapsin I-associated phosphatidylinositol 3-kinase mediates synaptic vesicle delivery to the readily releasable pool. J. Biol. Chem. *278*, 29065–29071.

Domin, J., Pages, F., Volinia, S., Rittenhouse, S. E., Zvelebil, M. J., Stein, R. C., and Waterfield, M. D. (1997). Cloning of a human phosphoinositide 3-kinase with a C2 domain that displays reduced sensitivity to the inhibitor wortmannin. Biochem. J. *326*, 139–147.

Eberhard, D. A., Cooper, C. L., Low, M. G., and Holz, R. W. (1990). Evidence that the inositol phospholipids are necessary for exocytosis. Loss of inositol phospholipids and inhibition of secretion in permeabilized cells caused by a bacterial phospholipase C and removal of ATP. Biochem. J. *268*, 15–25.

Falasca, M., Hughes, W. E., Dominguez, V., Sala, G., Fostira, F., Fang, M. Q., Cazzolli, R., Shepherd, P. R., James, D. E., and Maffucci, T. (2007). The role of phosphoinositide 3-kinase C2α in insulin signaling. J. Biol. Chem. *282*, 28226–28236.

Gaidarov, I., Smith, M. E., Domin, J., and Keen, J. H. (2001). The class II phosphoinositide 3-kinase C2alpha is activated by clathrin and regulates clathrin-mediated membrane trafficking. Mol. Cell *7*, 443–449.

Gaidarov, I., Zhao, Y., and Keen, J. H. (2005). Individual phosphoinositide 3-kinase C2alpha domain activities independently regulate clathrin function. J. Biol. Chem. *280*, 40766–40772.

Gillooly, D. J., Morrow, I. C., Lindsay, M., Gould, R., Bryant, N. J., Gaullier, J. M., Parton, R. G., and Stenmark, H. (2000). Localization of phosphatidylinositol 3-phosphate in yeast and mammalian cells. EMBO J. *19*, 4577–4588.

Hayakawa, A., Hayes, S. J., Lawe, D. C., Sudharshan, E., Tuft, R., Fogarty, K., Lambright, D., and Corvera, S. (2004). Structural basis for endosomal targeting by FYVE domains. J. Biol. Chem. *279*, 5958–5966.

James, D. J., Khodthong, C., Kowalchyk, J. A., and Martin, T.F.J. (2008). Phosphatidylinositol 4,5-bisphosphate regulates SNARE-dependent membrane fusion. J. Cell Biol. *182*, 355–366.

Johnson, E. E., Overmeyer, J. H., Gunning, W. T., and Maltese, W. A. (2006). Gene silencing reveals a specific function of hVps34 phosphatidylinositol 3-kinase in late versus early endosomes. J. Cell Sci. *119*, 1219–1232.

Kong, A. M. *et al*. (2006). Phosphatidylinositol 3-phosphate [PtdIns(3)P] is generated at the plasma membrane by an inositol polyphosphate 5-phosphatase: endogenous PtdIns(3)P can promote GLUT4 translocation to the plasma membrane. Mol. Cell. Biol. *26*, 6065–6081.

Lindmo, K., and Stenmark, H. (2006). Regulation of membrane traffic by phosphoinositide 3-kinases. J. Cell Sci. *119*, 605–614.

Matthew, W. D., Tsavaler, L., and Reichardt, L. F. (1981). Identification of a synaptic vesicle-specific membrane protein with a wide distribution in neuronal and neurosecretory tissue. J. Cell Biol. *91*, 257–269.

Meunier, F. A., Feng, Z. P., Molgo, J., Zamponi, G. W., and Schiavo, G. (2002). Glycerotoxin from *Glycera convoluta* stimulates neurosecretion by up-regulating N-type Ca^{2+} channel activity. EMBO J. *21*, 6733–6743.

Meunier, F. A., Osborne, S. L., Hammond, G. R., Cooke, F. T., Parker, P. J., Domin, J., and Schiavo, G. (2005). Phosphatidylinositol 3-kinase C2α is essential for ATP-dependent priming of neurosecretory granule exocytosis. Mol. Biol. Cell *16*, 4841–4851.

Milosevic, I., Sorensen, J. B., Lang, T., Krauss, M., Nagy, G., Haucke, V., Jahn, R., and Neher, E. (2005). Plasmalemmal phosphatidylinositol-4,5-bisphosphate level regulates the releasable vesicle pool size in chromaffin cells. J. Neurosci. *25*, 2557–2565.

Osborne, S. L., Meunier, F. A., and Schiavo, G. (2001). Phosphoinositides as key regulators of synaptic function. Neuron *32*, 9–12.

Osborne, S. L., Wallis, T. P., Jimenez, J. L., Gorman, J. J., and Meunier, F. A. (2007). Identification of secretory granule phosphatidylinositol 4,5-bisphosphate-interacting proteins using an affinity pulldown strategy. Mol Cell Proteomics *6*, 1158–1169.

Osborne, S. L., Wen, P. J., Boucheron, C., Nguyen, H. N., Hayakawa, M., Kaizawa, H., Parker, P. J., Vitale, N., and Meunier, F. A. (2008). PIKfyve negatively regulates exocytosis in neurosecretory cells. J. Biol. Chem. *283*, 2804–2813.

Osborne, S. L., Wen, P. J., and Meunier, F. A. (2006). Phosphoinositide regulation of neuroexocytosis: adding to the complexity. J. Neurochem. *98*, 336–342.

Panaretou, C., and Tooze, S. A. (2002). Regulation and recruitment of phosphatidylinositol 4-kinase on immature secretory granules is independent of ADP-ribosylation factor 1. Biochem. J. *363*, 289–295.

Pattni, K., Jepson, M., Stenmark, H., and Banting, G. (2001). A PtdIns(3)P-specific probe cycles on and off host cell membranes during *Salmonella* invasion of mammalian cells. Curr. Biol. *11*, 1636–1642.

Patton, C., Thompson, S., and Epel, D. (2004). Some precautions in using chelators to buffer metals in biological solutions. Cell Calcium *35*, 427–431.

Petiot, A., Faure, J., Stenmark, H., and Gruenberg, J. (2003). PI3P signaling regulates receptor sorting but not transport in the endosomal pathway. J. Cell Biol. *162*, 971–979.

Razzini, G., Brancaccio, A., Lemmon, M. A., Guarnieri, S., and Falasca, M. (2000). The role of the pleckstrin homology domain in membrane targeting and activation of phospholipase Cβ(1). J. Biol. Chem. *275*, 14873–14881.

Stein, M. P., Feng, Y., Cooper, K. L., Welford, A. M., and Wandinger-Ness, A. (2003). Human VPS34 and p150 are Rab7 interacting partners. Traffic *4*, 754–771.

Vanhaesebroeck, B., Leevers, S. J., Ahmadi, K., Timms, J., Katso, R., Driscoll, P. C., Woscholski, R., Parker, P. J., and Waterfield, M. D. (2001). Synthesis and function of 3-phosphorylated inositol lipids. Annu. Rev. Biochem. *70*, 535–602.

Vergne, I., Chua, J., and Deretic, V. (2003). Tuberculosis toxin blocking phagosome maturation inhibits a novel Ca^{2+}/calmodulin-PI3K hVPS34 cascade. J. Exp. Med. *198*, 653–659.

Vitale, N., Gensse, M., Chasserot-Golaz, S., Aunis, D., and Bader, M. F. (1996). Trimeric G proteins control regulated exocytosis in bovine chromaffin cells: sequential involvement of Go associated with secretory granules and Gi3 bound to the plasma membrane. Eur. J. Neurosci. *8*, 1275–1285.

Wendler, F., Page, L., Urbe, S., and Tooze, S. A. (2001). Homotypic fusion of immature secretory granules during maturation requires Syntaxin 6. Mol. Biol. Cell *12*, 1699–1709.

Wiedemann, C., Schafer, T., and Burger, M. M. (1996). Chromaffin granule-associated phosphatidylinositol 4-kinase activity is required for stimulated secretion. EMBO J. *15*, 2094–2101.

Zhang, J., Banfic, H., Straforini, F., Tosi, L., Volinia, S., and Rittenhouse, S. E. (1998). A type II phosphoinositide 3-kinase is stimulated via activated integrin in platelets. A source of phosphatidylinositol 3-phosphate. J. Biol. Chem. *273*, 14081–14084.

Zhao, Y., Gaidarov, I., and Keen, J. H. (2007). Phosphoinositide 3-kinase C2{α} links clathrin to microtubule-dependent movement. J. Biol. Chem. *282*, 1249–1256.